The results of thermal design/analyses performed on the 300 corner Laser Ranging Retro-Reflector (LRRR 300) to determine array operating temperature levels, net array/lunar environment heat exchange, and corner optical performance profiles are contained herein. The entire LRRR thermal design effort is described commencing with the concept thermal evaluation (PDR), leading to a parametric study for design optimization (Δ PDR), and a final analysis verification to support the candidate thermal design selection (CDR).

Thermal/optical design adequacy of the LRRR 300 configuration is analytically confirmed by conformance to Exhibit B-1, "Design and Performance Specification for the Laser Ranging Retro-Reflector Experiment", revised 1 November 1970.

Thermal analysis and design of the LRRR 300 was authorized under BxA CCP-269 to contract NAS 9-5829.

Prepared by E. Granholm
E. Granholm

Approved by J. M. Brueger
J. M. Brueger

TABLE OF CONTENTS

LIST OF FIGURES

LIST OF TABLES

1.0 INTRODUCTION

The 300 corner array has evolved from the first generation 100 corner arrays so as to increase optical return intensity levels. The LRRR 300 concept thermal evaluation (PDR) indicated that optical return levels were somewhat marginal and that the intended optical performance objective had not been fully realized. Therefore, thermal/design/analysis efforts were directed toward determining techniques which would improve optical return levels.

An LRRR 300 thermal design meeting was held on 28 October at BxA with NASA and Dr. Faller (PI) to select a heat transfer scheme which optimizes array thermal/optical performance. Several candidates were examined, and the preferred solution was to remove the multi-layer insulation bags from both arrays and to apply Z-93 white thermal coating directly to the ribbed array structure and sides.

Compared to previous LRRR thermal designs, the approach is basically different. Therefore, further verification of the candidate design selection was provided by a detailed thermal/optical analysis effort.

2.0 SUMMARY

Removal of the multi-layer insulation, employed on previous 100 corner LRRR's, and application of IIT's Z-93 to the array rear surfaces and sides was analytically confirmed to be the optimum LRRR 300 thermal/optical design. Table I highlights the results of the final thermal analysis corresponding to the Hadley Rille site.

TABLE I

HIGHLIGHTS OF FINAL LRRR 300 THERMAL ANALYSIS

Description	Value
Maximum Array Temperature	169°F
Minimum Array Temperature	-320°F
Optical Return Profile	for 80% of lunar cycle optical return is above 80%
Minimum Optical Return	67%

The Apollo 11 LRRR (EASEP) has been subjected to thermal/vacuum qualification testing (Reference 2) at environmental temperature levels of -320°F to +250°F and at a surrounding pressure of 5 x 10^{-6} torr. Test results indicated thermal integrity for the EASEP configuration, whose array composite is nearly identical to LRRR 300.

Thermal analysis data (Reference 3) consisting of lunar environment heat loads and array element temperatures were transmitted to ADL so that optical return intensity levels could be determined. The ADL generated optical profile meets and exceeds thermal/optical design requirements defined in paragraph 3.1.5 "Thermal Control" of Reference 4, which is outlined below:

> "The temperature gradient maintained across any reflector during 75% of the lunar cycle... shall be such that the return light intensity... be at least 80%... . The minimum return at any time during the lunar cycle shall be no less than 30%... ."

Conformance to the above thermal/optical design requirements provides a level of confidence that the LRRR 300 will perform satisfactorily when deployed at the Hadley Rille landing site.

3.0 THERMAL ANALYSIS TECHNIQUES

Thermal analysis of the LRRR 300 was accomplished by the BxA Thermal Analyzer Program (BTAP) which solves a mathematical/thermal model representing the physical configuration. The program generates temperature distributions and heating rates for either steady-state or transient conditions.

The lunar cycle was assumed to be sufficiently long (29.5 days) so that boundary conditions were considered constant which enabled steady-state thermal analyses to be employed. Solar angles of particular interest corresponding to corner break-through points, array noon, etc., were individually investigated using the "quasi" steady-state approach.

The LRRR 300 mathematical/thermal model contains discrete nodal points to define the array composite and leveling leg assembly. Dimensions and materials used in determining thermal resistances were obtained in the Reference 5 drawings. Optical properties of IIT's Z-93 inorganic thermal coating were assumed to be 0.2 for solar absorptance and 0.9 for infrared emittance.

Boundary conditions, describing the lunar thermal environment, were represented by three nodal points - the shadowed lunar surface, the sunlit lunar surface, and space. LRRR radiation interchange factors to the shadowed and sunlit portions of the lunar surface were calculated at each solar angle investigated. The sunlit lunar surface equatorial temperature profile (Reference 6) was adjusted to the Hadley Rille latitude of 25° by the relationship:

$$T = Te \cos \theta^{1/4},$$

where

T = surface temperature(°R),
Te = equatorial surface temperature (°R), and
θ = latitude angle (degrees).

Lunar surface optical properties were assumed to be 0.95 for solar absorbtance and 1.0 for infrared emittance.

4.0 CONCEPT THERMAL EVALUATION (PDR)

4.1 Analysis

The analyzed LRRR 300 configuration is presented in Figure 1 which shows the package orientation on the lunar surface corresponding to the Hadley Rille landing site specified in Reference 1. The Hadley Rille site is at comparatively high latitude of 25^{o} while previous LRRR thermal investigations have considered an equatorial deployment site.

Thermal optical performance for the LRRR 300 is dependent upon deployment site, solar incidence angles, surface optical properties and a rather complex heat exchange network between the array, leveling leg, the shadowed and sunlit lunar surface, and space. Multilayer insulation, attached to the lateral and bottom surfaces of the arrays, is covered by Beta cloth to provide protection against LM ascent plume heating. The leveling leg is coated with Z-93 white, inorganic thermal paint.

The simplified LRRR 300 concept thermal/mathematical model contains 9 nodal points to define the arrays, leveling leg, and environmental boundary conditions. Nodal numbers and associated descriptions are presented below:

Nodal Number	Description
1	204 Corner array
2	96 corner array
3	204 array insulation
4	96 array insulation
5	Structure assembly
6	Sun Compass
98	Shadowed lunar surface
99	Sunlit lunar surface
100	Space

4.2 Results

Major differences between LRRR 300 and earlier LRRR designs are principally the increased array surface area necessary to accommodate 300 corner reflectors and the method of array/structure attachment. Figure 2 presents a comparison of Apollo 14 LRRR and LRRR 300 arrays-to-structure mounting

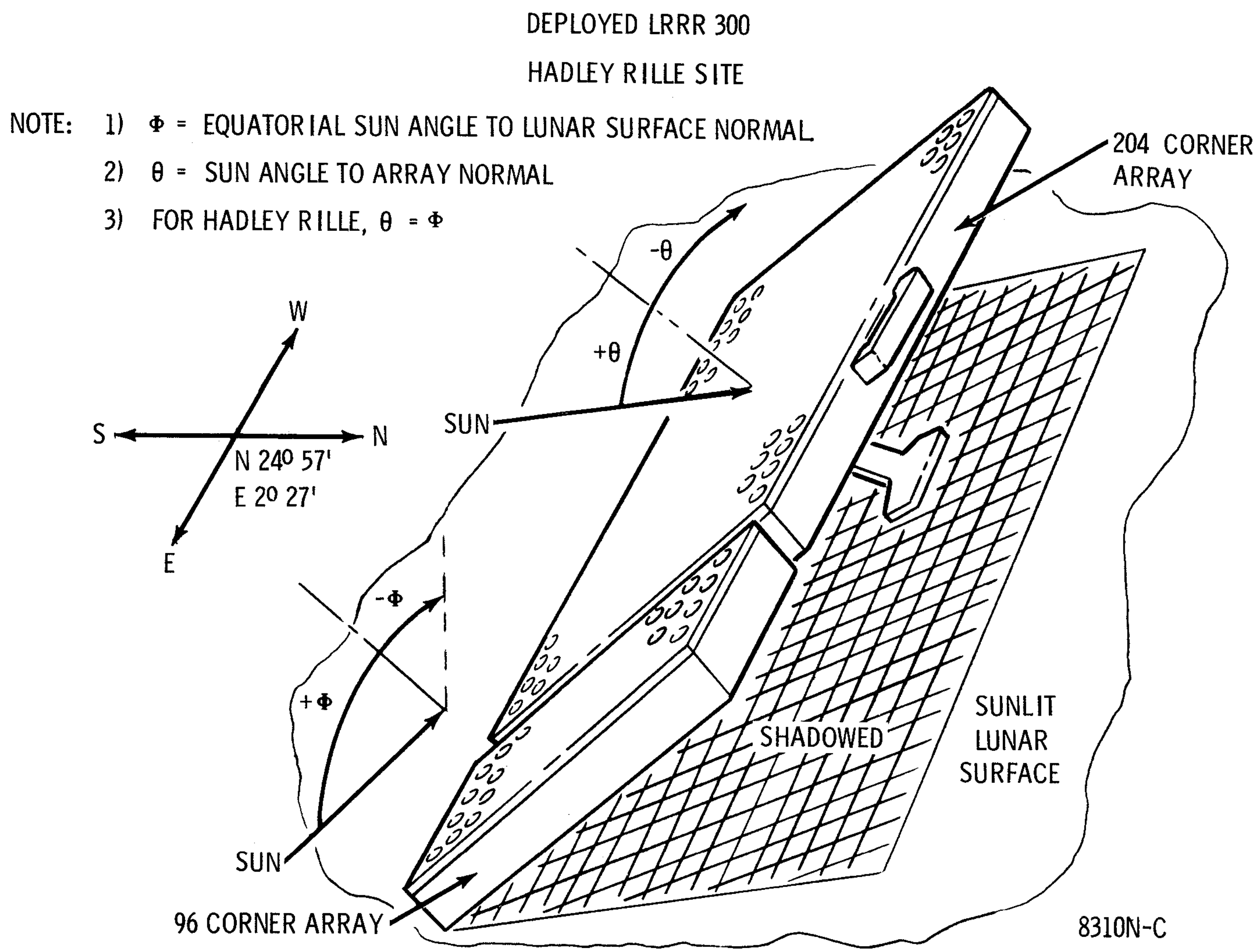
DEPLOYED LRRR 300
HADLEY RILLE SITE
NOTE: 1) Φ = EQUATORIAL SUN ANGLE TO LUNAR SURFACE NORMAL
2) θ = SUN ANGLE TO ARRAY NORMAL
3) FOR HADLEY RILLE, θ = Φ
W
S
N
E
N 24° 57'
E 2° 27'
-θ
+θ
SUN
204 CORNER ARRAY
-Φ
+Φ
SUN
SHADOWED
SUNLIT LUNAR SURFACE
96 CORNER ARRAY
8310N-C

Figure 1

APOLLO 14 AND PDR LRRR 300 ARRAY/STRUCTURE ATTACHMENT

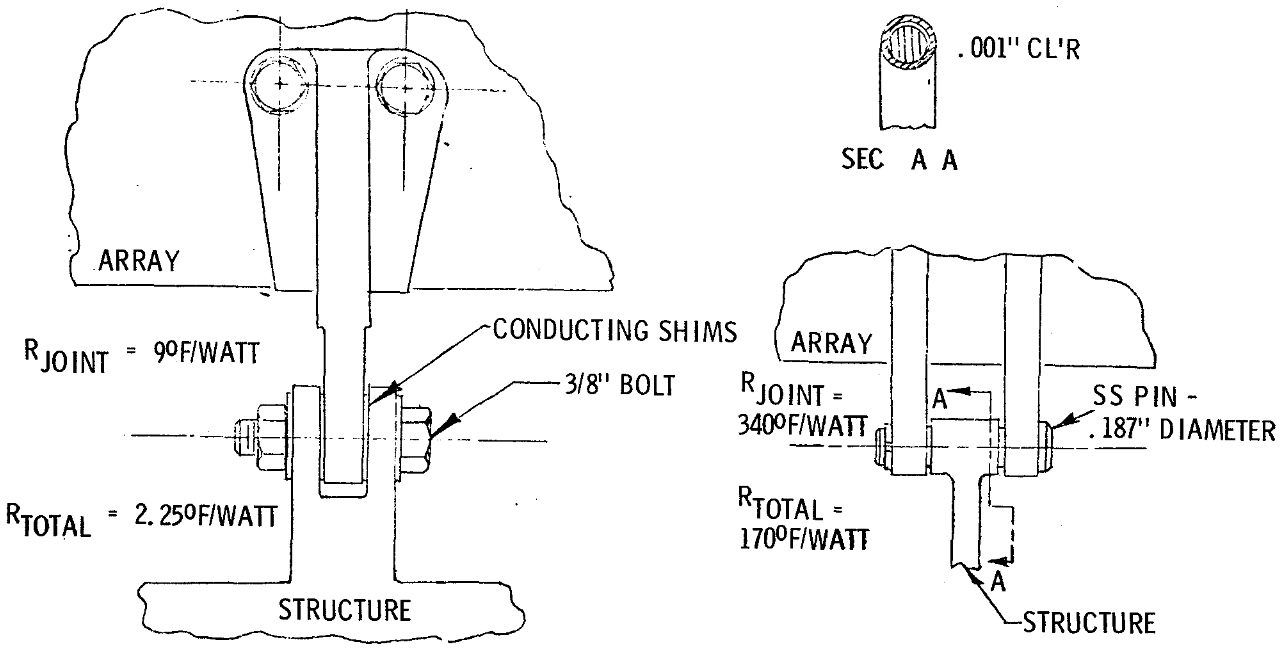

APOLLO 14 BOLTED JOINT (RIGID)

LRRR 300 PINNED JOINT (FLEXIBLE)

8310N-D

Figure 2

schemes. It is noted that on a per-joint basis, thermal resistance associated with the LRRR 300 attachment is approximately 38 times higher than that for Apollo 14. Since there are twice as many joints for Apollo 14, four as compared with two, the equivalent total thermal resistance for the LRRR 300 array/structure mounting interface is approximately 75 times higher than the corresponding value for Apollo 14. In short, multilayer insulation and the high thermal resistance joints act to decouple the LRRR 300 arrays from lunar surface thermal effects.

A comparison of array temperature profiles for LRRR 300 and Apollo 14, shown in Figure 3, demonstrates the aforementioned decoupling occurrance. Maximum array temperatures for the LRRR 300 and Apollo 14 are 210°F and 183°F respectively. The higher array temperature results from the impedance of heat flow from the array to the relatively cooler shadowed lunar surface. The lower LRRR 300 array temperature of 53°F is due to the blockage of heat flow into the array from the hotter lunar surface. LRRR 300 temperature levels are detailed in Table II.

Given in Figure 4 is the heat absorbed per array cavity from the structure and through the array insulation for various solar angles. The array/lunar surface decoupling phenomenon for LRRR 300 is graphically illustrated by the greatly reduced net heat flow into and out of the array. Maximum heat absorbed and rejected on a per cavity basis for Apollo 14 is 230 mw and 330 mw, respectively. Corresponding values for LRRR 300 are 17 mw and 35 mw, respectively.

Figure 5 presents a direct comparison of ADL generated relative central irradiance data reflecting the structure heating influence on the array for Apollo 14 and LRRR 300. Generally, the LRRR 300 represents a degraded thermal/optical design since the values of relative central irradiance are below those for the Apollo 14 design. The LRRR 300 optical return is above 80% for approximately 67% of the lunar cycle and the minimum return is 30%.

For Apollo 14, the optical return is above 80% for 90% of the lunar cycle and the minimum optical return at any time is 63%.

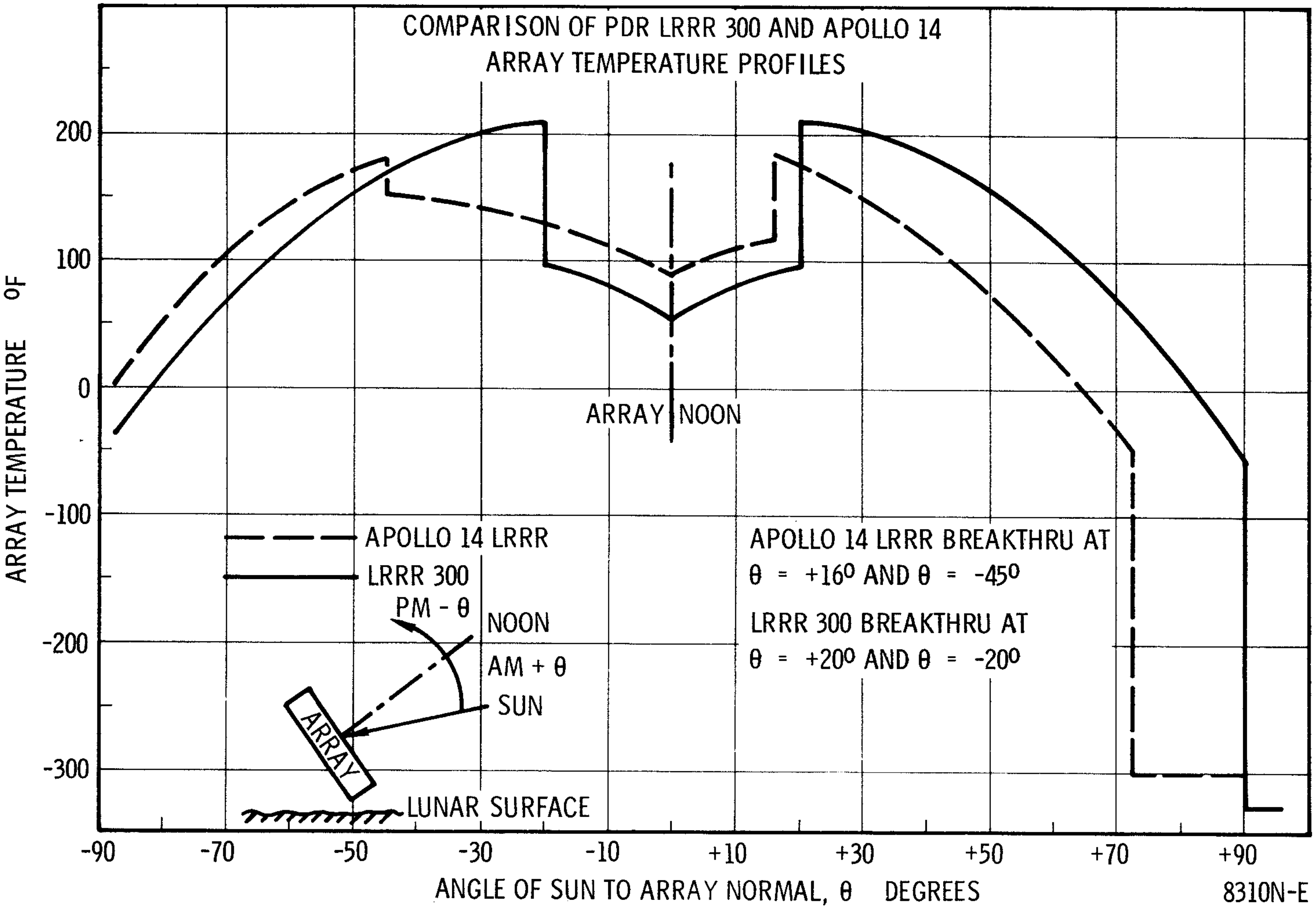
COMPARISON OF PDR LRRR 300 AND APOLLO 14
ARRAY TEMPERATURE PROFILES
ARRAY TEMPERATURE °F
200
100
0
-100
-200
-300
ARRAY NOON
APOLLO 14 LRRR
LRRR 300
APOLLO 14 LRRR BREAKTHRU AT
θ = +16° AND θ = -45°
LRRR 300 BREAKTHRU AT
θ = +20° AND θ = -20°
PM - θ
NOON
AM + θ
SUN
ARRAY
LUNAR SURFACE
-90
-70
-50
-30
-10
+10
+30
+50
+70
+90
ANGLE OF SUN TO ARRAY NORMAL, θ DEGREES
8310N-E

Figure 3

LRRR 300 - PDR TEMPERATURE LEVELS

Description	"204" Array Temp ~ °F	"96" Array Temp ~ °F	"204"Array Ins Temp ~°F	"96" Array Ins Temp ~°F	Leg Assy Temp ~°F	Comp Assy Temp ~ °F	Shadow Temp ~ °F	Sunlit Temp ~ °F
Lunar Night, $\theta > 90^{\circ}$	-330	-334	-320	-327	-323	-328	-300	N/A
Lunar Sunrise, $\theta = 90^{\circ}$	-252	-206	-205	-68	-201	-248	N/A	-206
Mid-Morning, $\theta = \pm 45^{\circ}$	172	172	60	43	-32	90	43	170
AM Brkthru, $\theta = \pm 20^{\circ}$	210	210	116	96	17	135	111	218
Post AM Brkthru, $\theta = \pm 20^{\circ}$	96	96	114	94	14	131	111	218
Lunar Noon, $\theta = 0$	53	52	132	111	30	142	135	233
Lunar Sunset, $\theta = -90^{\circ}$	-222	-247	-116	-197	-165	-224	N/A	-182

TABLE II

COMPARISON OF PDR LRRR 300 AND APOLLO 14 ARRAY HEAT ABSORPTION PROFILES

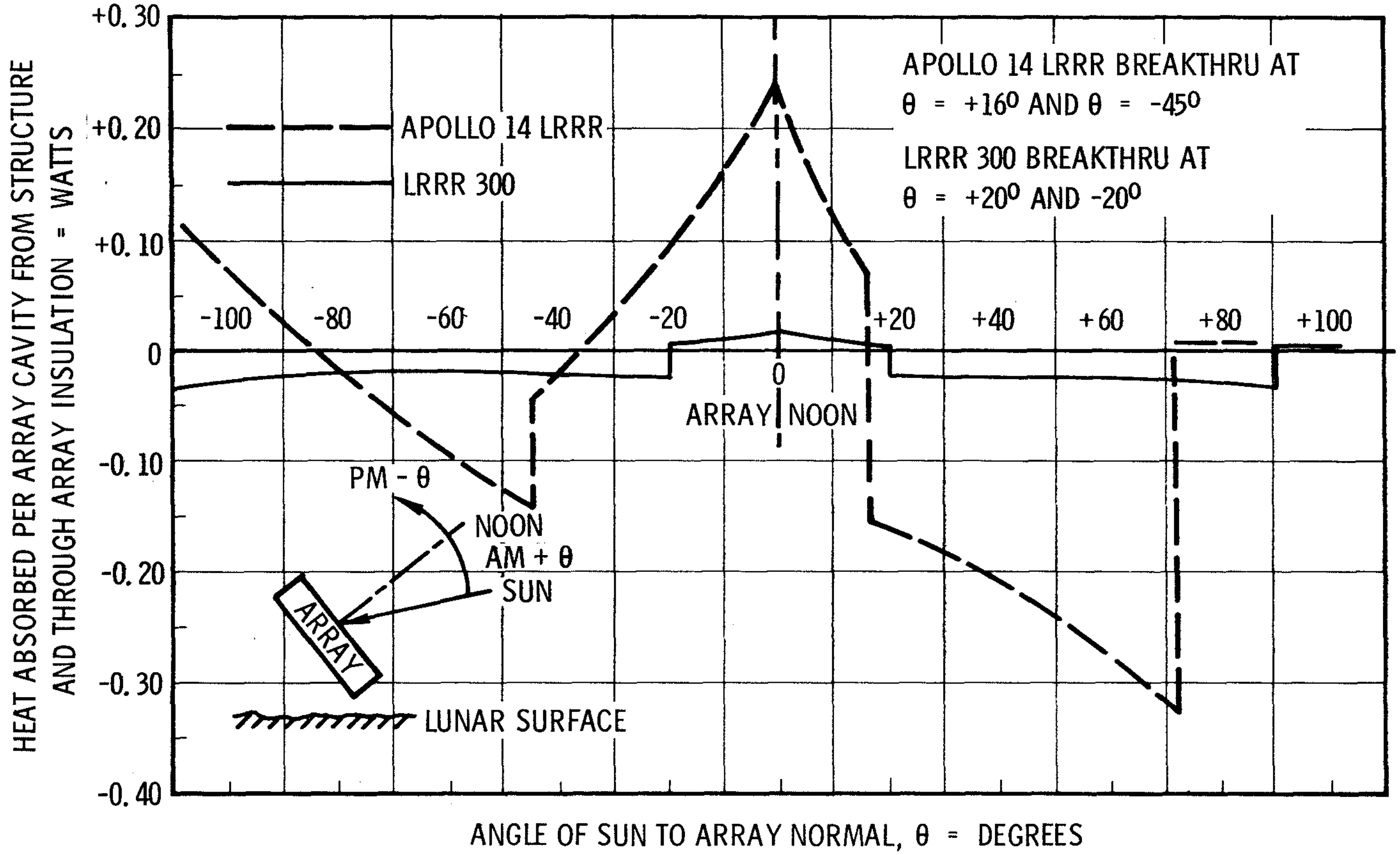

Figure 4

COMPARISON OF PDR LRRR 300 AND APOLLO 14 RELATIVE CENTRAL IRRADIANCE PROFILES

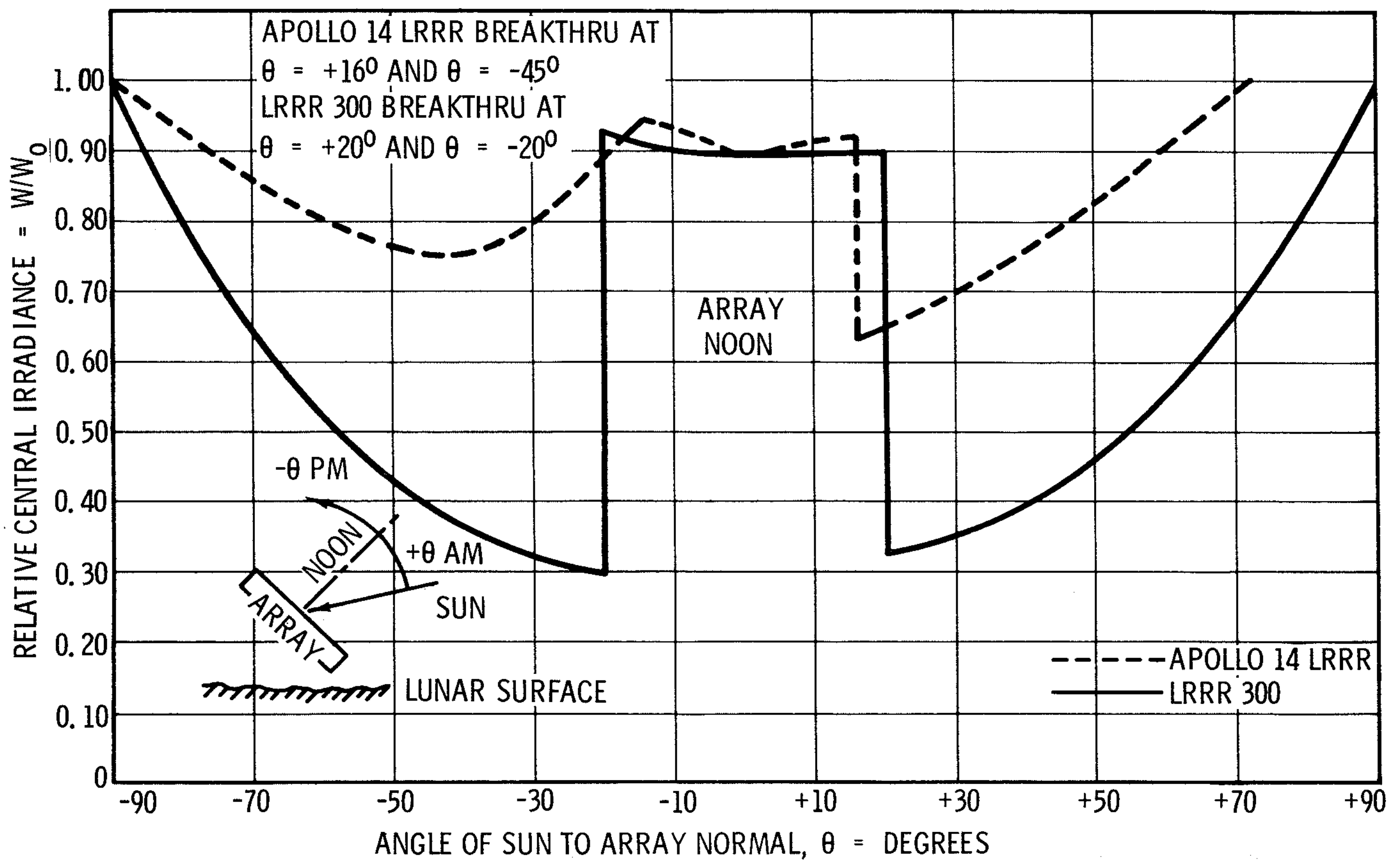

8310N-G

Figure 5

4.3 PDR Conclusions and Recommendations

The results of the LRRR 300 concept thermal analysis indicate that the estimated thermal optical performance does not meet the design criteria specified in Reference 4, (previously stated in the summary section). Maximum temperature levels are less than the Reference 2 maximum allowable level of 250°F. However, from an overall thermal standpoint, the present LRRR 300 heat transfer design could be considerably improved.

Coupling the LRRR 300 arrays to the lunar surface will enhance mutual heat interchange and effect an overall improvement in optical return levels. Array heat transfer to the relatively cool lunar surface during early morning and late afternoon portions of the lunar cycle represents an optical design improvement. If heat flow out of the array could be increased from 35 mw/cavity to 200 mw/cavity, which is feasible, an improvement in relative central irradiance from 0.5 to 0.7 would be accomplished. Heat flow into the array during the lunar noon interval when the array is cool due to total internal reflection of solar energy will result in a slightly degraded optical return. However, the noon interval is brief and the optical return can still be maintained above 80%.

5.0 THERMAL DESIGN OPTIMIZATION (Δ PDR)

5.1 Analysis

Thermal analysis prior to PDR utilized a mathematical model which combined all array elements into one node and assigned the array effective properties of solar absorptance and infrared emittance as defined in Figure 6. The solution was a reiterative process since the effective emittance is a function of heat gained or rejected through the array rear surface, which is initially unknown and must be assumed. The analytical technique, although accurate, was awkward and too slow to be employed in a parametric study in which execution of many cases was required.

Upon request of BxA, ADL supplied a simplified version of their detailed radiosity network, as shown in Figure 6. The model enabled BxA to calculate temperature levels of discrete array elements and heat transfer interaction between elements. ADL also supplied solar heating profiles which were applied at nodes corresponding to the array structure, the optical corner, and the corner retaining ring. The revised thermal/mathematical model of the array surface provided a rigorous and accurate analytical tool for use in the post-PDR parametric study.

At PDR, it was decided that any design change to improve LRRR 300 optical performance could not be deployment site dependent, but must be an effective solution for all potential landing sites. For this reason, two landing sites were examined - Hadley Rille because it is prime and Marius Hills as it is secondary. Presented in Figure 7 are the coordinate systems for each site. At Hadley Rille the sun plane is approximately parallel to the array/leveling leg hinge line and the sun never directly illuminates the array rear surface. However, at Marius Hills, the sun plane is approximately perpendicular to the array/leveling leg hinge line and the sun illuminates the array rear surface for $58^{\circ}/360^{\circ}$ or 16% of the lunar cycle. By coincidence, the primary and secondary sites are representative of the range of lunar environmental conditions imposed on the array. Therefore, if a common solution can be found for Hadley Rille and Marius Hills, it can be reasoned that the same solution would be valid for any potential lunar landing site.

Shown in Table III are relative central irradiance data for three heat load levels and the two sites. Optical return values are defined at various solar angles to the array normal and are consistent with the Figure 7 coordinate systems. Heat transfer to (or from) the array rear surface is initially simulated by constant heat loads for which relative central irradiance data is computed by ADL. When the actual heat transfer rates through the array rear surface are determined, they are interpolated between existing constant heating values to yield an actual optical return profile.

LRRR 300 - ARRAY FRONT SURFACE THERMAL/MATH MODELS

PDR THERMAL/MATH MODEL

ONE NODE, COMBINED ARRAY ELEMENTS

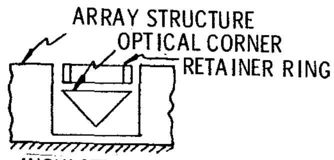

EFFECTIVE THERMAL/OPTICAL PROPERTY DEFINITION

$$\alpha EFF = \frac{\Sigma P_F}{SA_A \cos\theta}, \text{ WHERE}$$

αEFF = EFFECTIVE SOLAR ABSORPTANCE,
ΣP_F = SUMMATION OF POWERS INTO ARRAY FRONT SURFACE,
S = SOLAR CONSTANT,
A_A = ARRAY SURFACE AREA, AND
θ = ANGLE OF SUN WITH RESPECT TO ARRAY NORMAL.

ϵEFF

$$\epsilon EFF = \frac{\Sigma P_F + \Sigma P_R}{A_A \sigma T_A^4}, \text{ WHERE}$$

ϵEFF = EFFECTIVE INFRARED EMITTANCE,
ΣP_R = SUMMATION OF POWERS INTO ARRAY REAR SURFACE,
σ = STEFAN-BOLTZMANN CONSTANT, AND
T_A = TEMPERATURE OF ARRAY.

ΔPDR THERMAL/MATH MODEL

FIVE NODE RADIOSITY NETWORK

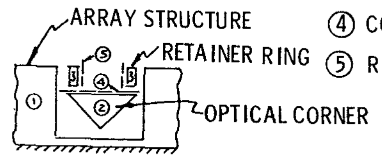

RADIOSITY NETWORK THERMAL CONDUCTANCES

	NODE CONNECTIONS	CONDUCTANCE	
CONSTANT	1-2	0.6517 CM^2	
	1-2	0.005 W/°K	
	1-3	0.005 W/°K	
	2-3	0.005 W/°K	
	2-4	71.15 CM^2	
	3-5	96.60 CM^2	
	4-5	7.126 CM^2	
SITE DEPENDENT	1 - SP. MOON	0.108 CM^2	TOTAL
	4 - SP. MOON	5.431 CM^2	
	5 - SP. MOON	9.781 CM^2	

SOLAR HEATING PROFILES ARE INPUT DIRECTLY INTO NODES 1, 2, AND 3.

8310N-H

Figure 6

LRRR 300
DEPLOYMENT SITE COORDINATE SYSTEMS

HADLEY RILLE SITE
(N 24° 57', E 2° 27')

MARIUS HILLS SITE
(N 14° 46', W 56° 33')

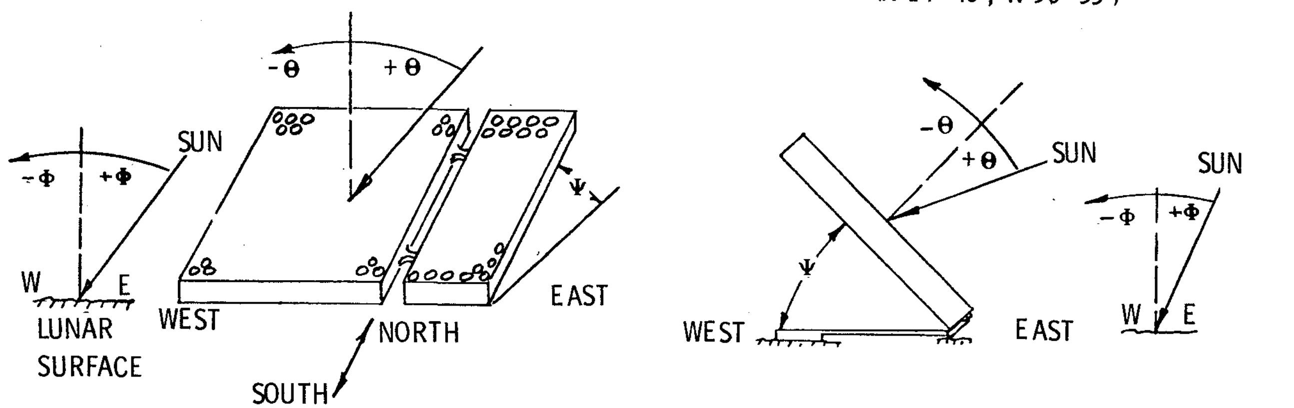

Hadley Rille Site:

Ψ = ARRAY TILT ANGLE = 25°

Φ = ANGLE OF SUN TO LUNAR SURFACE NORMAL

θ = ANGLE OF SUN TO ARRAY NORMAL

$$\theta = \Phi$$

Marius Hills Site:

Ψ = ARRAY TILT ANGLE = 58°

Φ = ANGLE OF SUN TO LUNAR SURFACE NORMAL

θ = ANGLE OF SUN TO ARRAY NORMAL

$$\theta = \Phi - \Psi$$

$$\theta = \Phi - 58^0$$

8310N-I

Figure 7

LRRR 300
PARAMETRIC RELATIVE CENTRAL IRRADIANCE DATA
HADLEY RILLE SITE

θ ~ Degrees	W/Wo 100W In	W/Wo 0W In/Out	W/Wo 100W Out
72.5	0.70	0.90	0.95
40.0	0.30	0.30	0.78
30.0	0.30	0.30	0.70
20.0	0.30	0.81	0.88
0	0.40	0.93	0.82
-20.0	0.30	0.92	0.87
-30.0	0.30	0.30	0.70
-50.0	0.30	0.45	0.92
-72.5	0.60	0.90	0.99

MARIUS HILLS SITE

θ ~ Degrees	W/Wo 100W In	W/Wo 0W In/Out	W/Wo 100W Out
30.0	0.30	0.30	0.72
28.0	0.30	0.80	0.86
20.0	0.35	0.88	0.83
0	0.47	0.91	0.75
-18.0	0.33	0.90	0.80
-20.0	0.30	0.30	0.80
-40.0	0.30	0.40	0.92
-60.0	0.30	0.85	0.90
-72.5	0.75	0.87	0.77
-90.0	0.90	0.84	0.60
-119.0	0.90	0.84	0.60
-148.0	0.90	0.84	0.60

TABLE III

From Table III, optical return in most instances increases as heat flow out of the array rear surface increases. During the lunar cycle when the sun illuminates the array front surface, the structure is typically hotter than the corners, making array heat removal beneficial to optical performance. At Marius Hills when the sun illuminates the array rear surface, the array is cooler than the optical corners and limited heat addition to the array can actually improve optical performance. Therefore, it appears that coupling the array rear surface to lunar environmental surroundings can be an effective solution for optimizing optical return at both potential landing sites.

Presented in Figure 8 are various thermal design candidates allowing radiative heat transfer between the array rear surface, the lunar surface, and space. The magnitude of array/lunar environment coupling is highest for Configuration 1, and decreases for ascending configuration numbers.

5.2 Results

For Configuration 1, the multi-layer insulation bags were removed from both arrays and the array ribbed structure was coated with Z-93 white thermal paint. Figure 9 shows relative central irradiance profiles corresponding to the LRRR 300 PDR concept configuration and Configuration 1 for the Hadley Rille and Marius Hills landing sites. At both sites, Configuration 1 represents a considerable thermal design improvement over the PDR configuration. Configuration 1 optical performance is above 0.80 for approximately 79% of the lunar cycle, and the minimum return is 0.58 at Hadley Rille. For Marius Hills the estimated optical return profile is above 0.80 for virtually the entire lunar cycle. Reference 4 thermal/optical guidelines, which were specified earlier, have now been met at both sites.

A comparison made between the four thermal design candidates for Hadley Rille and Marius Hills is presented in Figure 10. Configurations 2, 3, and 4 demonstrate optical performance profiles inferior to Configuration 1, but none exhibit an optical return profile lower than that of the PDR configuration. It is seen that high coupling efficiency between the array and lunar environment maximizes optical return levels.

Shown in Figure 11 are LRRR 300 array temperature profiles for Hadley Rille and Marius Hills. Removal of the multi-layer insulation will reduce maximum array temperature levels for Hadley Rille and Marius Hills to 160°F and 168°F, respectively. Minimum array temperatures occur just prior to lunar sunrise and are approximately -310°F for both sites.

LRRR 300
THERMAL DESIGN CANDIDATES

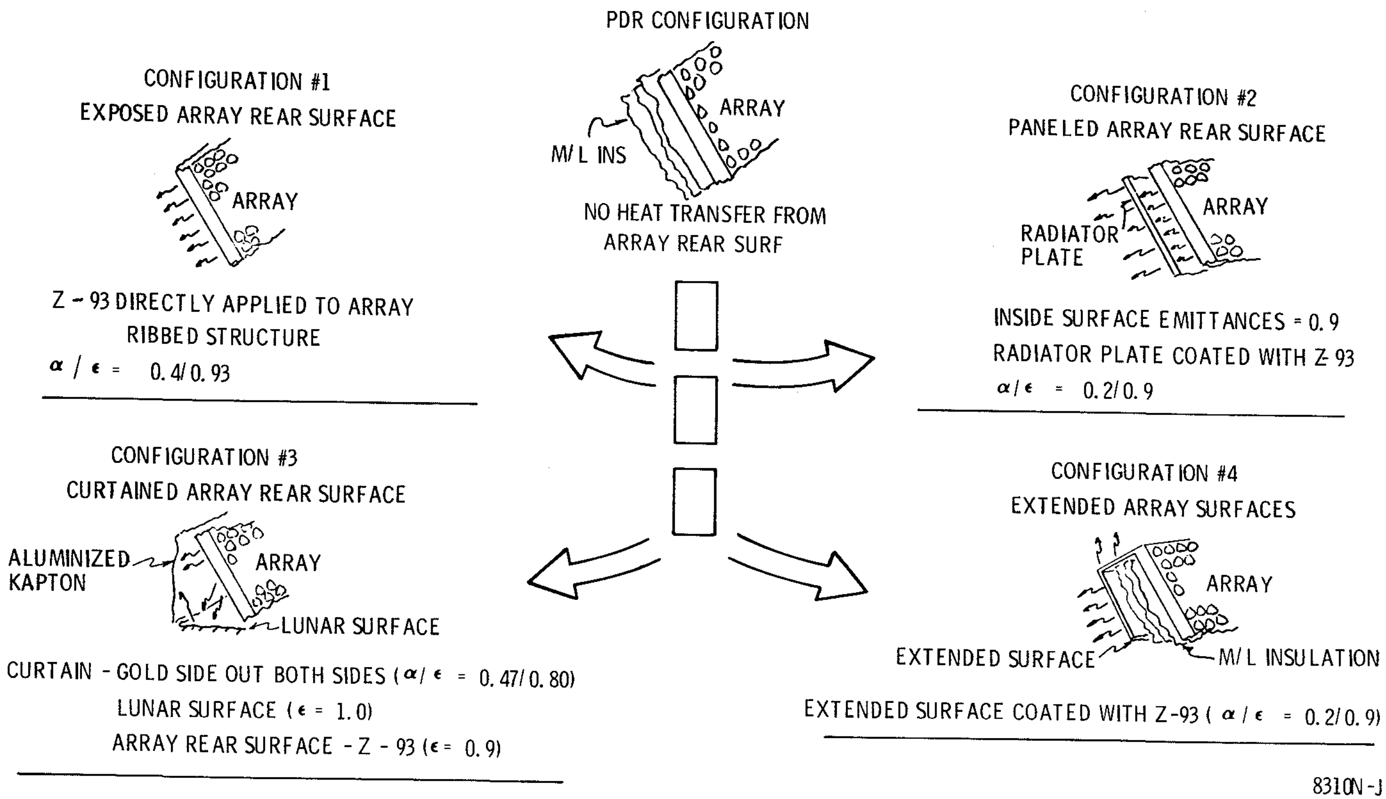

Figure 8

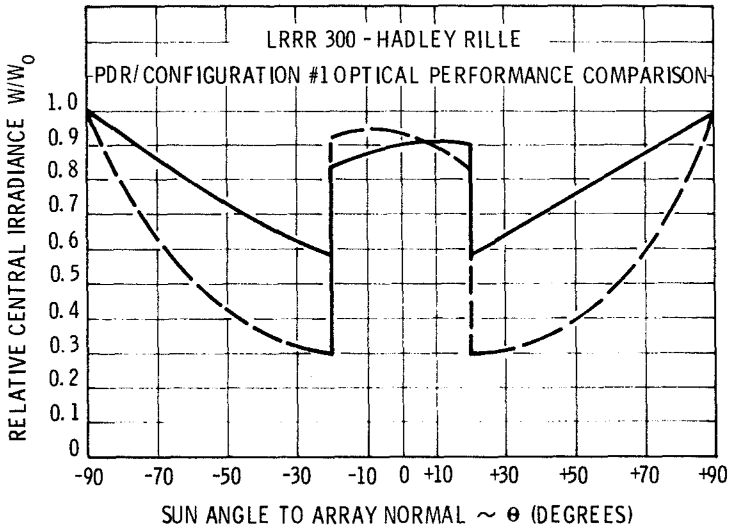

PDR CONFIGURATION

— — — INSULATION BAG INSTALLED (67% OF LUNAR CYCLE, OPTICAL PERFORMANCE IS ABOVE 0.80)

CONFIGURATION #1

——— INSULATION BAG REMOVED, Z-93 COATING DIRECTLY APPLIED TO ARRAY REAR SURFACE (79% OF LUNAR CYCLE, OPTICAL PERFORMANCE IS ABOVE 0.80)

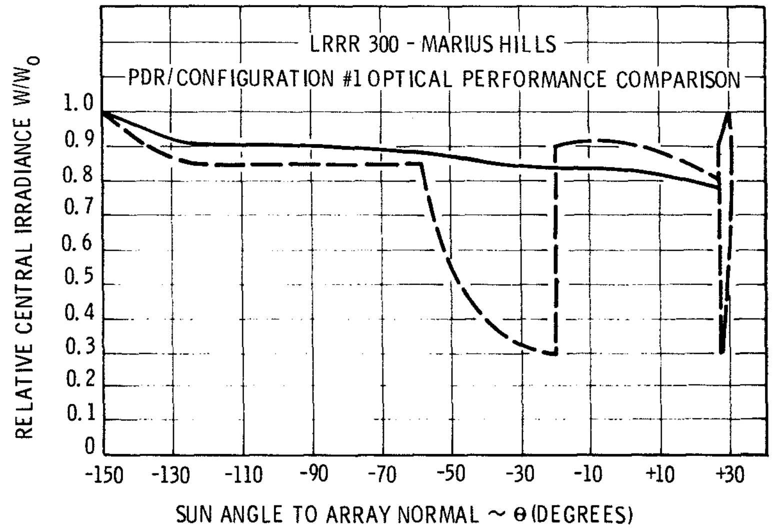

PDR CONFIGURATION

— — — INSULATION BAG INSTALLED (87% OF LUNAR CYCLE OPTICAL, PERFORMANCE IS ABOVE 0.80)

CONFIGURATION #1

——— INSULATION BAG REMOVED, Z-93 COATING DIRECTLY APPLIED TO ARRAY REAR SURFACE (VIRTUALLY 100% OF LUNAR CYCLE, OPTICAL PERFORMANCE IS ABOVE 0.80)

8310N-K

Figure 9

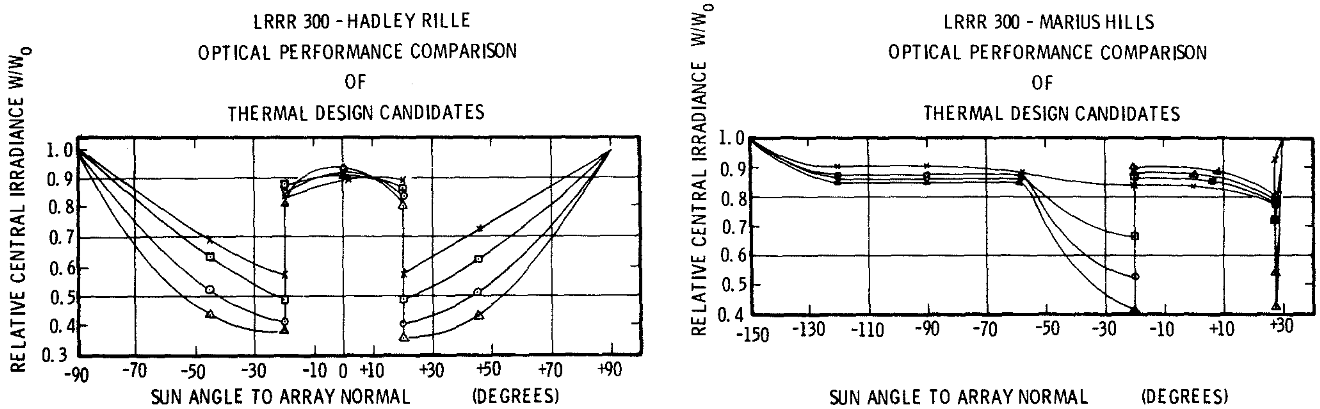

X CONFIG 1, EXPOSED ARRAY REAR SURFACE (79% OF LUNAR CYCLE ABOVE 0.8)
⊡ CONFIG 2, PANELED ARRAY REAR SURFACE (75% OF LUNAR CYCLE ABOVE 0.8)
⊙ CONFIG 3, CURTAINED ARRAY REAR SURFACE (71% OF LUNAR CYCLE ABOVE 0.8)
△ CONFIG 4, EXTENDED ARRAY SURFACES (68% OF LUNAR CYCLE ABOVE 0.8)

X CONFIG 1, EXPOSED ARRAY REAR SURFACE (VIRTUALLY 100% OF LUNAR CYCLE ABOVE 0.8)
⊡ CONFIG 2, PANELED ARRAY REAR SURFACE
⊙ CONFIG 3, CURTAINED ARRAY REAR SURFACE
△ CONFIG 4, EXTENDED ARRAY SURFACES
} APPROX 90% OF LUNAR CYCLE ABOVE 0.8)

8310N-M

Figure 10

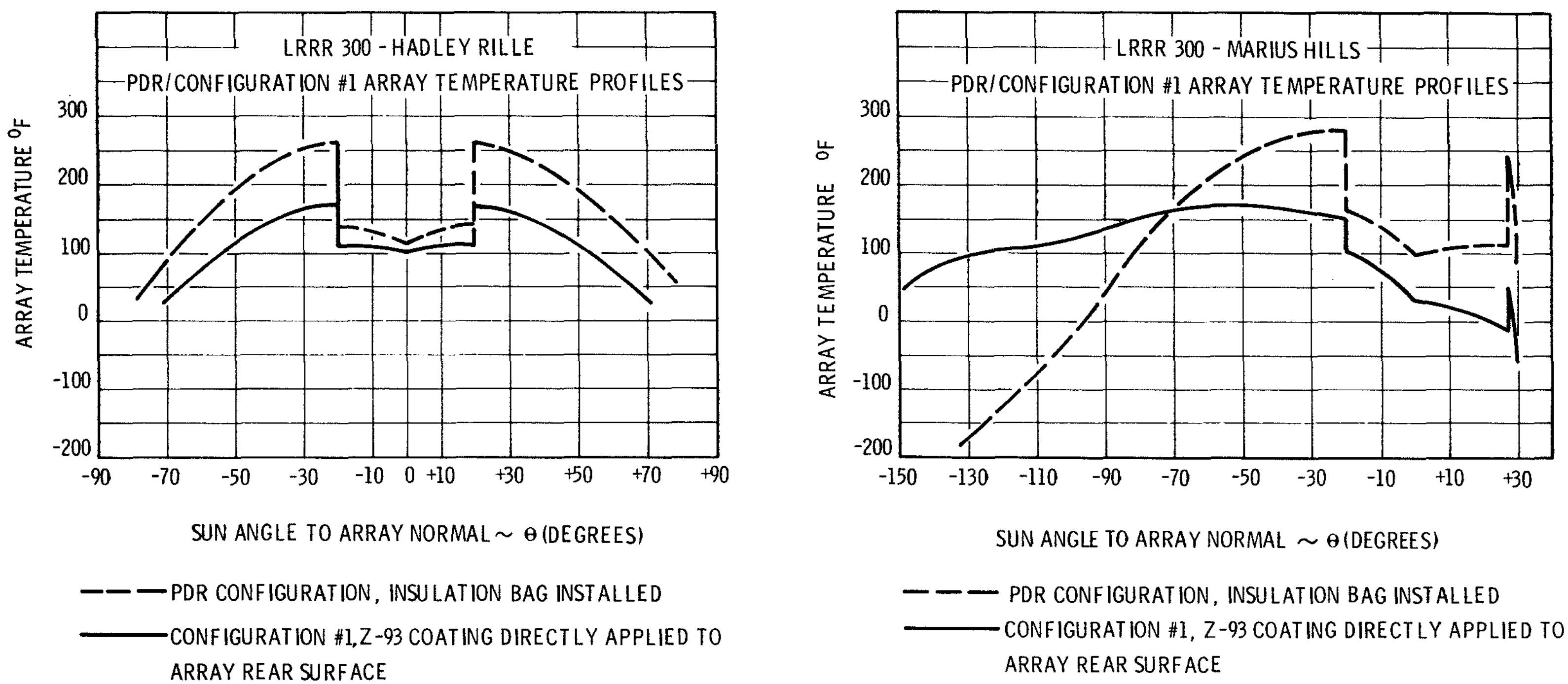

Figure 11

8310N-L

5.3 Recommendations and Conclusions

Based upon the findings of the Δ PDR study, Configuration 1, as defined in Figure 8, represents the most effective solution for increasing LRRR 300 optical return levels. The following advantages can be realized with the Configuration 1:

1) superior optical performance at any potential lunar landing site,

2) reduced array structure maximum temperature levels,

3) minimum difficulty of implementation into existing mechanical design, and

4) no impact on LRRR 300 total weight (actually a slight weight savings).

It is therefore recommended that the multilayer insulation bags be eliminated and the LRRR 300 array rear surfaces and sides be painted with IIT's Z-93 white thermal control coating.

6.0 DESIGN VERIFICATION THERMAL ANALYSIS (CDR)

6.1 Analysis

The LRRR 300 thermal control scheme of insulation removal and utilization of Z-93 thermal coating was incorporated into the mechanical design on 28 October. A final LRRR 300 thermal/mathematical model corresponding to the Hadley Rille landing site and reflecting the revised thermal/optical design was generated to define, in detail, heat transfer rates and temperature levels essential for a final optical performance prediction. The previously employed LRRR 300 model was, by necessity, simple to permit rapid evaluation of several thermal control concepts. The final model permits a rigorous thermal analysis of the experiment by accounting in detail for thermal effects such as solar heating of the array sides, temperature difference between arrays, cavity effects of the array ribbed surfaces, and shadowing as a function of solar angle.

The LRRR 300 physical configuration was sub-divided into nodal points as shown in Table 4:

TABLE IV

LRRR 300 FINAL THERMAL MODEL

Node Number	Description
1	"204" array structure
2	"204" array corners
3	"204" array retainer rings
4	"204" corner radiation shields
5	"204" ring radiation shields
6	"96" array structure
7	"96" array corners
8	"96" array retainer rings
9	"96" corner radiation shields
10	"96" ring radiation shields
98	Shadowed lunar surface, array rear side
99	Sunlit lunar surface, array rear side
100	Space, array rear side
101	Sunlit lunar surface, array front side
102	Space, array front side

Boundary nodes for the thermal network consisted of 99, 100, 101, and 102. Constant temperatures impressed on the sunlit lunar surface nodes (99 & 101) were extracted from Reference 6 and adjusted to 25° latitude as previous discussed in Section 3.0, Thermal Analysis Techniques. Radiation to space from all array elements was accomplished by using constant temperature nodes 100 and 102 which were maintained at -460.0°F.

Geometric view factors between the array rear surfaces, the shadowed and sunlit portions of the lunar surface, and space are shown in Figure 12. Shadow temperatures were calculated by the Thermal Analyzer Program at each solar angle investigated. The primary mode of heat rejection from the array rear surfaces is by radiation to the experiment shadow which in turn radiates to space. The LRRR 300 shadow provides an efficient heat exchange surface between the array structure and space. Limited array heat rejection is possible by direct radiation to space.

6.2 Results

Results of LRRR 300 detailed heat transfer analysis were documented in Reference 3 and transmitted to ADL on 17 November so that optical performance could be accurately predicted by digital computer techniques. The transmitted thermal interface information consists of lunar environmental heat loads to be impressed on various array elements as a function of solar angle to the array normal. The data are presented in Table V.

HADLEY RILLE SITE SHADOW GEOMETRIC VIEW FACTORS

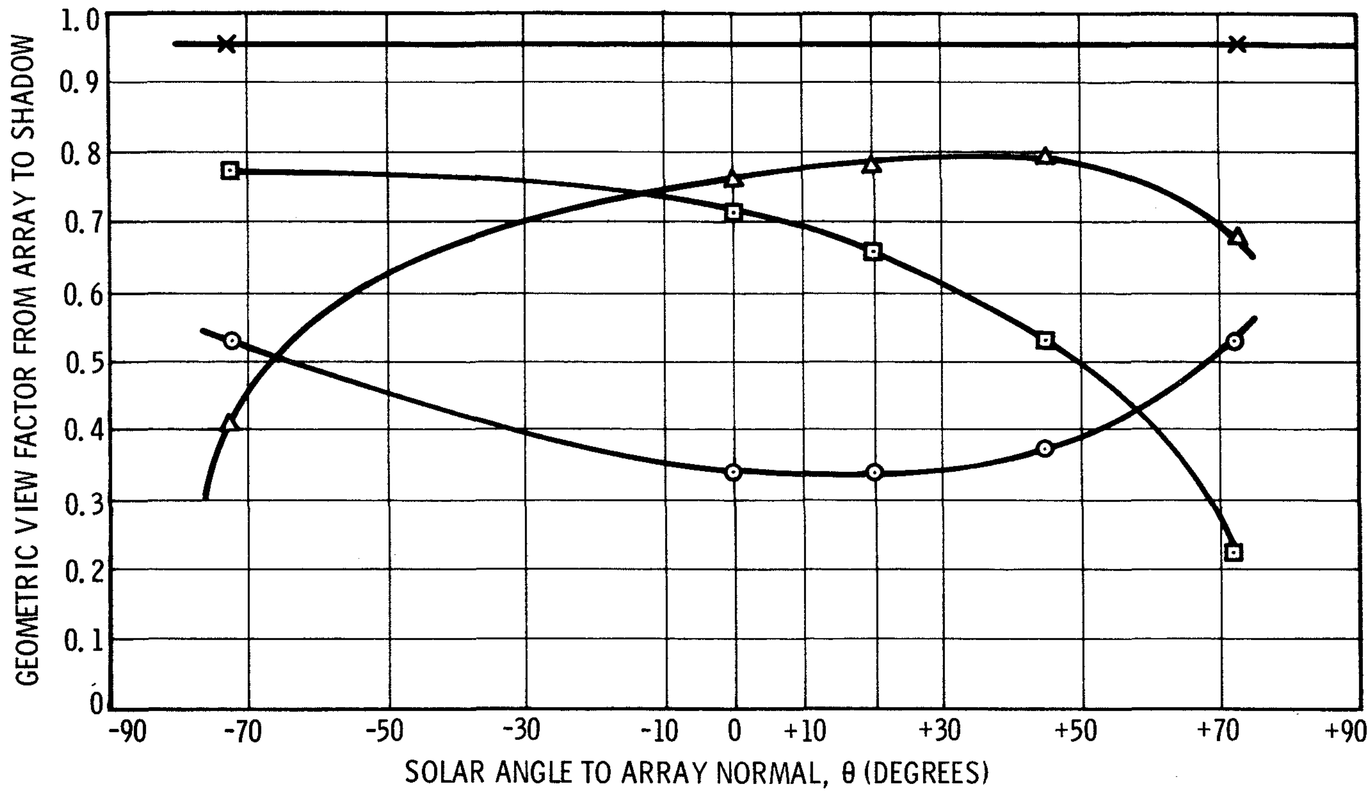

× VIEW FACTOR FROM ARRAYS TO ENTIRE LUNAR SURFACE
△ VIEW FACTOR FROM LARGE ARRAY TO SHADOW
□ VIEW FACTOR FROM SMALL ARRAY TO SHADOW
○ VIEW FACTOR FROM SHADOW TO SPACE

8310N-N

Figure 12

TABLE V

FINAL THERMAL INTERFACE INFORMATION

Angle of Sun to Array Normal, θ ~ Degrees	Array Structure Heat Load, Watts	Corner Shield Heat Load, Watts	Ring Shield Heat Load, Watts
Sunrise			
+72.5	-0.0320	+0.004	+0.00614
+40.0	-0.250	+0.0106	+0.0175
+30.0	-0.273	+0.0127	+0.0210
+20.0+	-0.286	+0.0145	+0.0242
+20.0-	-0.0423	+0.0184	+0.0323
0.0	+0.0343	+0.0228	+0.0416
-20.0+	-0.0423	+0.0184	+0.0323
-20.0-	-0.286	+0.0145	+0.0242
-30.0-	-0.270	+0.0128	+0.0208
-50.0	-0.215	+0.0085	+0.0142
-72.5	-0.0311	+0.00352	+0.00550
Sunset			

Instructions for ADL interpretation of the Table V data are presented in detail in Reference 3.

Table VI presents the results of final LRRR 300 thermal analyses. The table shows that for all solar angles except array noon (θ = 0), the array rear surfaces are able to reject heat to the lunar shadow, which is beneficial to optical performance. Total array rear surface heat absorption at noon is approximately 10 watts which will cause minimal degradation in optical return. Also from Table VI, array structure maximum and minimum temperature levels are 169°F and -320°F, respectively.

ADL final relative central irradiance data are shown in Table VII.

TABLE VII

ADL FINAL RELATIVE CENTRAL IRRADIANCE DATA

Array Sun Angle (degrees)	Relative Central Irradiance (%)	Array Sun Angle (degrees)	Relative Central Irradiance (%)
+90.0	100.0	-20.0+	92.1
+72.5	80.9	-20.0-	73.8
+40.0	72.4	-30.0	68.3
+30.0	68.6	-50.0	78.6
+20.0+	72.6	-72.5	80.9
+20.0-	92.1	-90.0	100.0
0.0	95.9		

Figure 13 presents a plot of ADL relative central irradiance data points and shows the most probable interpretation of the data using least-square curve fitting techniques. The extremities of the curve are hyperbolic functions of the form $y = \frac{1}{A+BX}$ and the central portion of the curve is parabolic function of the form $y = AX^2$. Maximum deviation of the fitted curve from the ADL data points is 6.8%. The relative central irradiance profile indicates that for 80 % of the lunar cycle the array optical return level is above 80%. Also, the minimum optical return at any time is 67%.

LRRR 300
RESULTS OF FINAL
THERMAL ANALYSIS

Sun Angle to Array Normal	204 Array/ Lunar Heat Transfer Rate (Watts)	96 Array/ Lunar Heat Transfer Rate (Watts)	204 Array Temperature (°F)	96 Array Temperature (°F)	Shadow Temperature (°F)	Sunlit Lunar Surf Temp (°F)
Lunar Night, $\theta > 90.0^\circ$	Negligible	Negligible	-320	-320	-300	-300
Early Morning, $\theta = 72.5^\circ$	16.6	6.1	-8	39	-83	53
Mid Morning & Mid Afternoon, $\theta = \pm 45.0^\circ$	55.6	24.2	119	143	58	170
Maximum Break-thru Heating, $\theta = \pm 20.0^\circ$	62.7	27.9	157	169	96	218
Reflecting Array, $\theta = \pm 20.0^\circ$	14.7	3.1	92	112	40	218
Array Noon, $\theta = 0$	-5.0	-5.2	77	85	24	233
Late Afternoon, $\theta = -72.5^\circ$	13.7	9.8	18	-15	-80	48

TABLE VI

FINAL LRRR 300 OPTICAL PERFORMANCE PROFILE
HADLEY RILLE

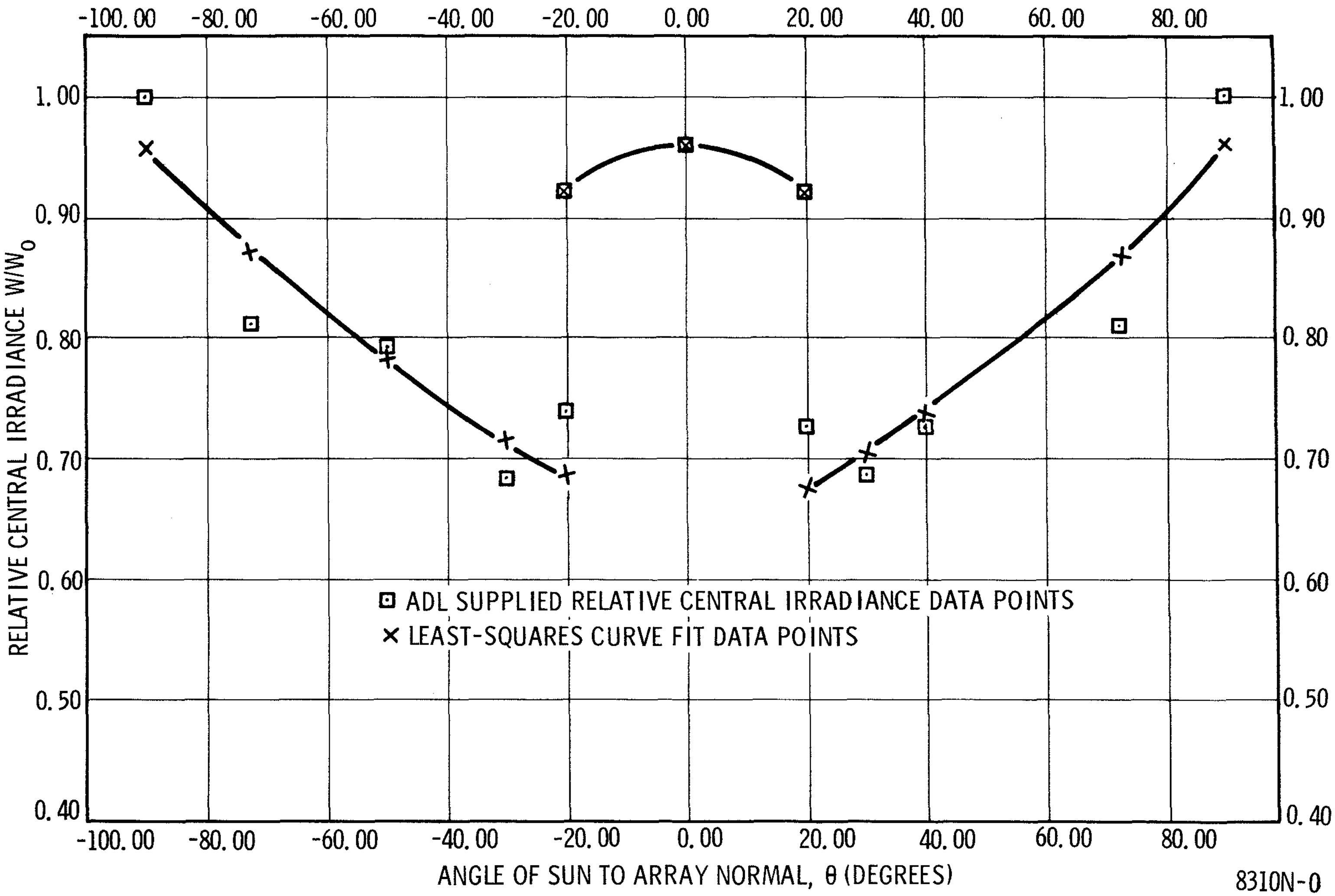

Figure 13

6.3 Final Conclusions

As previously stated in Section 2.0 (Summary), the revised LRRR 300 configuration, with multi-layer insulation removed and Z-93 thermal coating applied to the array rear and side surfaces, meets and exceeds thermal/optical requirements outlined in Reference 4. The maximum array temperature of 169°F is well below the qualification test upper-limit of 250°F as stated in Reference 2.

Therefore, the LRRR 300 thermal design is adequate and a level of confidence of successful optical performance at the Hadley Rille landing site has been established.

7.0 REFERENCES

1. Contact Report 978-951-046, "LRRR 300 Lunar Landing Sites", 9/3-4/70.

2. EATM-81, "LRRR Qualification Thermal/Vacuum Final Test Report", 4/25/69.

3. Memo 9712-99, "LRRR 300, Transmittal of Thermal Interface Information to Arthur D. Little, Inc.", 11/18/70.

4. Exhibit B-1, "Design and Performance Specification for the Laser Ranging Retro-Reflector Experiment", 3/4/70, revised 11/1/70.

5. Drawing Numbers 2347205 and 2347206, "Retro-Reflector Structure", Revision A.

6. Document No. LED-520-IF, "LM Design Criteria and Environments", 5/15/66.